Invited paper

Understanding of wet and alternative particle removal processes in microelectronics: theoretical capabilities and limitations

François Tardif, Adrien Danel, and Olivier Raccurt

Abstract—A 2 orders of magnitude range of van der Waals interactions is considered here to take the majority of the variety of shapes and materials of actual particles into account. Comparing these interactions with the repulsive forces generated by electrostatic charges, drag, surface tension, shock waves, high accelerations and aerosol particles, the intrinsic capabilities and limitations of the different cleaning processes can be predicted. Three kinds of particle-removal processes have been identified – universal processes capable of removing all particle sizes and types, even from patterned wafers, processes that present the same theoretical ability but are actually limited by the accessibility of the particles, and finally cleanings that are not able to remove all particle sizes.

Keywords— cleaning, SC1, particle removal.

1. Introduction

The continuous increase of IC integration density requires a reduction of both device dimensions and the corresponding amount of the material used. Consequently, the concentration of contaminants affecting the fabrication yield of very competitive microelectronic manufacturing is becoming smaller and smaller. Therefore, cleaning performance has to be continuously improved to remove the ultimate traces of contamination, such as particles, metals, organics, bases and anions.

According to the *International Technology Roadmap for Semiconductors* [1], smaller and smaller particle sizes will have to be eliminated as the device dimensions decrease: 50 nm as from 2004 and 10 nm in 2016.

Particles will probably be the most challenging type of contamination in the near future as the removal mechanism in the conventional Standard Clean 1 (SC1) [2] process is mainly based on a controlled consumption of the layer under the particle. But this consumption will be rapidly prohibited as the accuracy of the device dimensions (implantation, silicon on insulator, etc.) are now approaching the under-etching thicknesses required for particle removal.

In this work, fundamental particle-substrate interactions due to van der Waals, drag and surface tension forces, as well as electrostatic charges, are used to understand the intrinsic capabilities and limitations of the wet SC1 process and emerging new techniques such as explosive evaporation, high velocity sprays, acoustic waves, laser and cryogenic techniques.

2. Forces acting on particles

The main forces likely to be exerted on fine particles are calculated in Table 1. It can be seen from this table that the main four parameters that drive the particle adhesion/removal mechanisms are the electrostatic, van der Waals, capillary and drag forces [3].

Table 1
Orders of magnitude of the different forces acting on a 100 nm spherical particle in a solution with the density of 1

Forces	Order of magnitude (N)	Proportionality (R: Radius)
Van der Waals	10^{-7}	R
Electrostatic	10^{-8}	–
Capillary	10^{-8}	R
Drag (water, 10 m/s)	10^{-9}	R
Gravitation	10^{-16}	R^3
Archimedes	10^{-17}	R^3
Hydrostatic	10^{-21}	R^3

2.1. Capillary forces

The surface tension γ_{lg} is due to the cohesion between the molecules of the media and tends to minimize the interfacial areas. It represents a force per unit of interfacial length. In the case of the reference spherical particle, the maximum capillary force is obtained when the liquid wets the particle material perfectly and the gas/liquid interface is acting on the whole particle perimeter (see Fig. 1):

$$F_\gamma = 2\pi R \gamma_{lg} . \qquad (1)$$

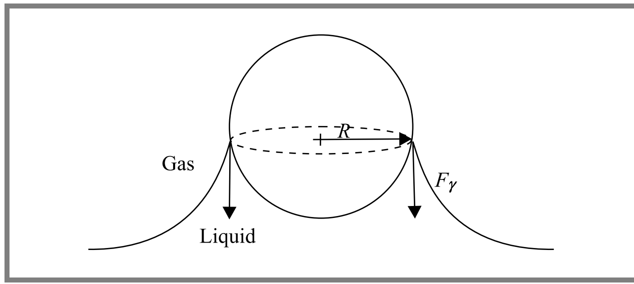

Fig. 1. Schematic of the maximum capillary force acting on a particle at a liquid/gas interface (case of contact angle = 0).

2.2. Drag forces

The viscosity of the moving fluids induces a drag force on the particles. In the case of a spherical particle of diameter D placed in a flow velocity V_p, this force is given with a good approximation [4] by the Stokes law up to the Reynolds number of ten[1]. In the case of a particle deposited on a surface, an additional constant of 1.7 accounting for the effect of the surface must be added [5]:

$$F_{Drag} = 1.7 \cdot 3\pi \mu D V_p \,, \tag{2}$$

where μ represents the fluid viscosity: 10^{-3} kg/m·s for water at 20°C.

This force is theoretically able only to push the particle in parallel to the surface. It can be expected that an asperity on the particle or on the substrate will transform this tangential force to a lift-off momentum [6]. In the case of non-spherical particles, the drag forces are generally higher.

2.3. Van der Waals forces

The particle-substrate attractions due to the van der Waals forces result from the dipole/dipole interactions between their constitutive molecules. These forces are so high that the particles are generally flattened on the substrate. The integration of the interactions between all the constitutive volume elements of a spherical particle or an infinite flat particle both on a perfectly flat substrate are given by (3) and (4), respectively:

$$F_{vdW} = \frac{AR}{6h^2} \,, \tag{3}$$

$$F_{vdW} = \frac{AS}{6\pi h^3} \,, \tag{4}$$

where: R – particle radius, h – particle-substrate distance (the minimum distance equal to the Lennard-Jones distance of $h_0 = 0.4$ nm for the considered materials), A – the Hamaker constant (depends on the particle, substrate materials and on the nature of the media: interaction transmission), S – facing particle and substrate surface.

[1]For a 100 nm particle, the Reynolds number of 10 corresponds to a water flow velocity of 100 m/s!

The Hamaker constants for different particle/substrate materials can be calculated using the data and the formula given by Israelachvili [7]. The results listed in Table 2 show that van der Waals forces for typical particle materials on SiO_2 substrates can vary by one order of magnitude depending on the media.

Table 2
Hamaker constants in water and in air calculated from reference [7]

Media	Al_2O_3/SiO_2	SiO_2/SiO_2	PSL/SiO_2
Water	$1.6 \cdot 10^{-20}$ J	$6.5 \cdot 10^{-21}$ J	$1.0 \cdot 10^{-20}$ J
Air	$9.6 \cdot 10^{-20}$ J	$6.3 \cdot 10^{-20}$ J	$7.5 \cdot 10^{-20}$ J

The difference between van der Waals attractions acting on the reference rigid and spherical particle and on actual particles is investigated here. The consequence of the non ideality of the actual particles: flattening, non specific shape, roughness, partially embedded, etc., can finally be considered as an additional flat surface in contact with the substrate.

In this work, the difference between the ideal and rigid sphere and the actual non-ideal particle is arbitrarily expressed by the fraction f equal to the surface in contact divided by the maximum surface that a particle of the same dimension is able to present πR^2:

$$f = \frac{S}{\pi R^2} \,. \tag{5}$$

In this way, f is null for an ideal particle and reaches 1 for a particle presenting the maximum surface in contact.

For a quasi-spherical particle presenting a small flat contact area, the total van der Waals forces can be considered as the sum of the contributions from the non-deformed particle and the contact surface [8] with the latter dominating the contribution from the spherical particle. Therefore, the ratio $\mathfrak{R}$ between the van der Waals attraction of the actual and the ideal (rigid and spherical) particles can be approximated by the equation:

$$\mathfrak{R} = \frac{\dfrac{AR}{6h^2} + \dfrac{AS}{6\pi h^3}}{\dfrac{AR}{6h^2}} = 1 + f\frac{R}{h} \,. \tag{6}$$

The results have been plotted in Fig. 2 for particle sizes ranging from 10 to 150 nm. It can be seen that the van der Waals forces increase rapidly with the non-ideality of the particles and can be more than 2 orders of magnitude higher than those for the ideal particle. This effect decreases with the particle size. Finally, due to a large variation range

of the Hamaker constant and considerable impact of the particle, van der Waals interactions can vary to a very large extent for the different existing particle types.

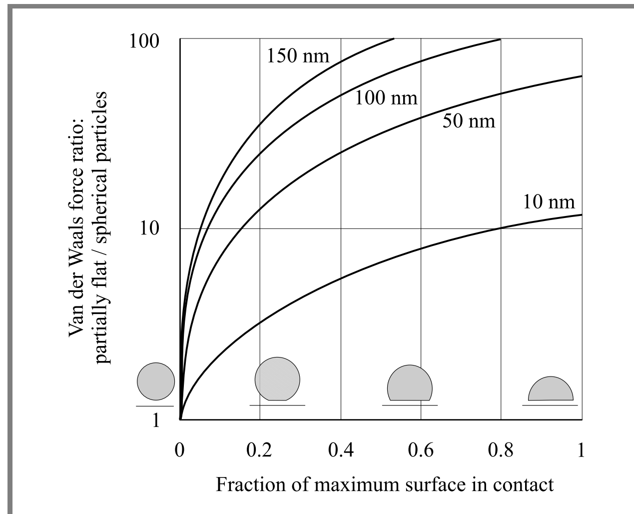

Fig. 2. Ratio $\mathfrak{R}$ between van der Waals forces calculated for the reference rigid sphere and particles presenting a flat surface in contact. This surface is given in percentage of the area of the sphere cross section which represents the maximum contact surface for a given particle size.

In this work, we arbitrarily chose to consider the van der Waals forces present in the system consisting of a rigid sphere of Al_2O_3 on SiO_2 substrate because its Hamaker constant is the highest of those listed in Table 2. In order to account for a shift from ideality, a range of the Hamaker constants of up to 2 orders of magnitude above the value mentioned above is considered. This approach enables a very wide majority of actually observed particles to be covered but clearly does not take into account the extreme cases of flat-shape particles made of materials exhibiting very high Hamaker constants.

The substrate roughness is not considered here as it generally decreases the contact areas leading to lower van der Waals interactions.

2.4. Force originating from electrostatic charges

Material surfaces usually present electrostatic charges that originate from ionization or dissociation of functional surface groups in chemical equilibrium with H^+ ions from the media (pH). In a liquid, a large number of charges are available close to the surface[2]. Ions carrying charge of the sign opposite to that of the surface (the counter ions) are immediately attracted to the surface, masking its surface potential until apparent neutrality is reached. As shown in Fig. 3, the surface charge density is characterized by the Zeta potential. This potential is due to the contributions from the particle charges and the retinue of counter ions sufficiently attached to the particle surface when it moves against the liquid (shear layer), e.g., under the influence of an electric field.

The thickness of the diffuse layer results from the competition between the electrostatic attraction exerted on the counter ions that build up at the charged surface and their re-diffusion to the bulk solution. A high temperature and a low ionic strength, therefore, enhance the diffuse layer thickness.

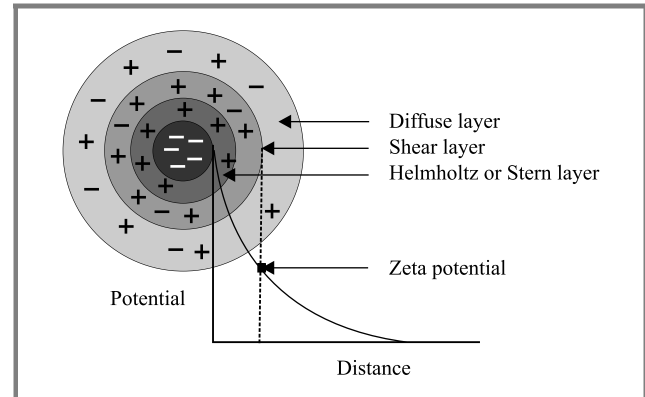

Fig. 3. Representation of a negatively charged particle dipped in an electrolyte.

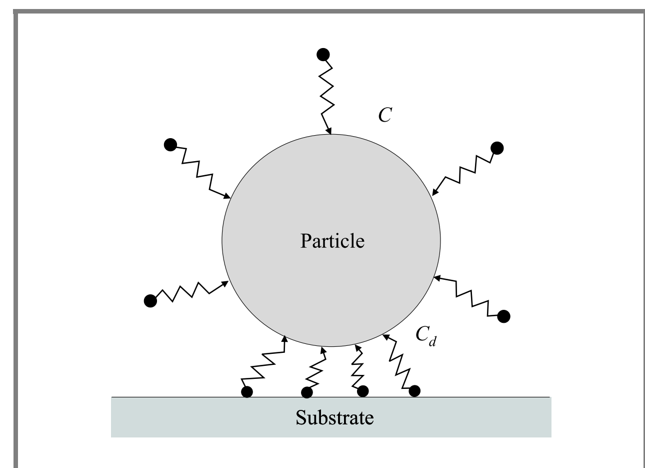

Fig. 4. Representation of a negative particle dipped in an electrolyte.

In fact, at very small particle/substrate distances, the major interactions caused by the charged surfaces are not due directly to the electrostatic forces but to the entropic contribution [9]. As shown in Fig. 4, the counter ion concentration is very high in between the particle and the substrate due to the overlap of the particle and substrate diffuse layers. This leads to the differential pressure between the top and bottom of the particle, expressed below:

$$F_e = (C_d - C)\,\mathrm{k}T\,, \qquad (7)$$

where: k – the Boltzmann constant, T – absolute temperature, C – concentrations.

[2]Even in the case of ultra pure water, there is a sufficient reservoir of H^+ and OH^- of 10^-7 mole/L.

Figure 5 shows the evolution of the Zeta potential versus pH for Si and SiO_2 as substrate materials and one of the most electropositive particle materials – alumina.

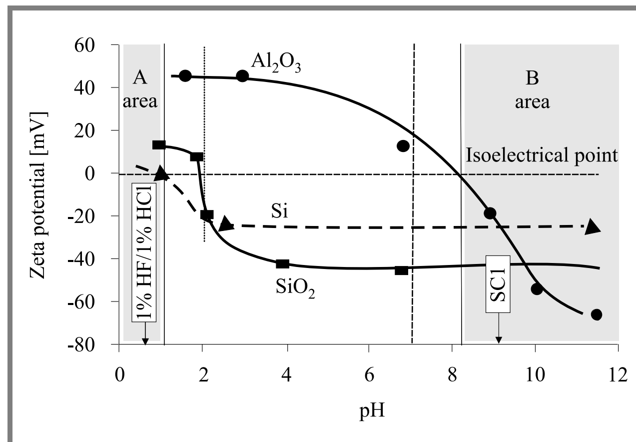

Fig. 5. Evolution of Al_2O_3, Si and SiO_2 Zeta potentials versus pH.

In order to facilitate particle removal and to prevent any re-deposition it is to be hoped that charges gathered on all particle types and on the substrate are of the same sign leading to electrostatic repulsion. This condition is fulfilled in both A and B areas.

The forces originating from electrostatic charges can be calculated by solving the Poisson-Boltzmann equation [7]. They are favored by:

– high absolute values of surface potential (same electrical sign), the area B is generally better in this respect than the area A;

– high ionic force (densification of the diffuse layer increasing the entropic force);

– high temperature (kT factor in Eq. (7)).

3. Particle removal mechanisms

Theoretical performances of conventional and prospective particle cleaning processes are discussed here.

3.1. Cleaning by etching and electrostatic repulsion

This cleaning mechanism consists in separating the particle from the substrate by consuming the substrate, the particles, or both, until the repulsive forces of electrostatic origin exceed the van der Waals forces. This means that the pH has to be adjusted in the area A or B. As shown in the example of Fig. 6, electrostatic forces decrease more slowly with the distance than van der Waals interactions. Therefore a liberation distance always exists regardless of the particle size and charge (theoretically 1.6 nm in the case of an ionic force of 0.5 M in Fig. 6).

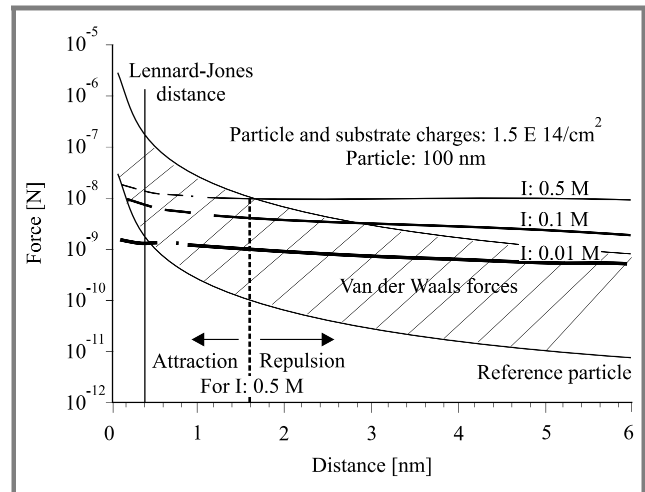

Fig. 6. Comparison between the order of magnitude of van der Waals forces (hatched area) and forces of electrostatic origin at different ionic strengths as a function of the separation distance. Calculations of van der Waals forces for distances lower than 0.4 nm and calculations of electrostatic forces for distances lower than 2 nm are not valid.

This theoretical etching thickness is increased in practice by the dynamic behavior of the removal process. Indeed, at the beginning of the separation, a competition occurs between the etching speed and the re-attraction speed of the particle due to van der Waals interactions (see Fig. 7).

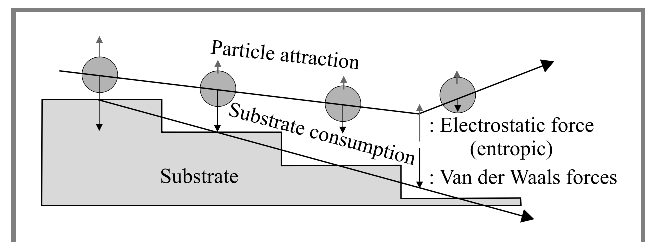

Fig. 7. Illustration of the dynamic behavior of the particle removal process by etching and electrostatic repulsion.

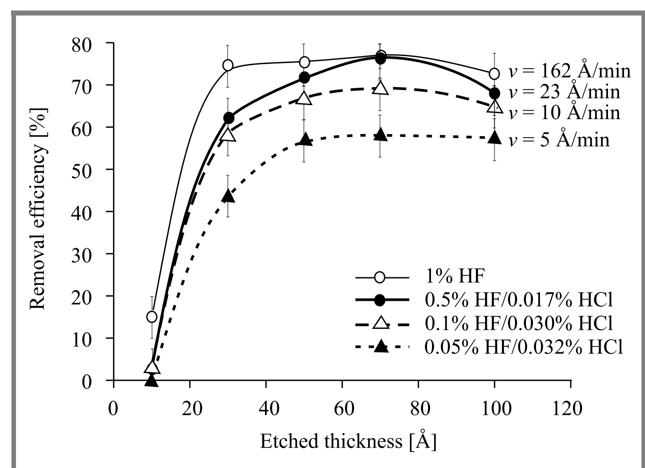

Fig. 8. Cleaning of 3000 SiO_2 particles deposited on a 200 mm SiO_2 substrate in HF solutions exhibiting different etching speeds (ionic strength and pH constant: 0.024 M and 1.4, respectively).

This phenomenon is verified in Fig. 8. When the etching speed is low, a higher material consumption is necessary to reach the nominal removal efficiency that is also lower. Particle removal processes, such as SC1 [2], IMEC clean [10], DDC [11, 12], etc., therefore have to present very fast etching kinetics. This requirement is compatible with the fast processes necessary for the new single wafer cleaning tools.

Particle removal by etching and electrostatic repulsion does not seem to present any limitation in terms of particle size since the necessary consumption of the material is acceptable. In practice, this amount can be limited by increasing the etching speed, the ionic force of the solution and absolute values of Zeta potentials.

3.2. Cleaning by drag forces

As shown in Fig. 9, drag forces induced by a continuous liquid jet are able to sweep along even very small particles. Nevertheless, very high pressures (50 bars) have to be used to have a chance of removing all particle types with a micro spray. In this calculation, we assume as the initial approximation that the thickness of the laminar boundary layer is zero just under the jet impact and that the order of magnitude of the drag force is approximated by (2). The jet therefore has to scan the whole wafer surface.

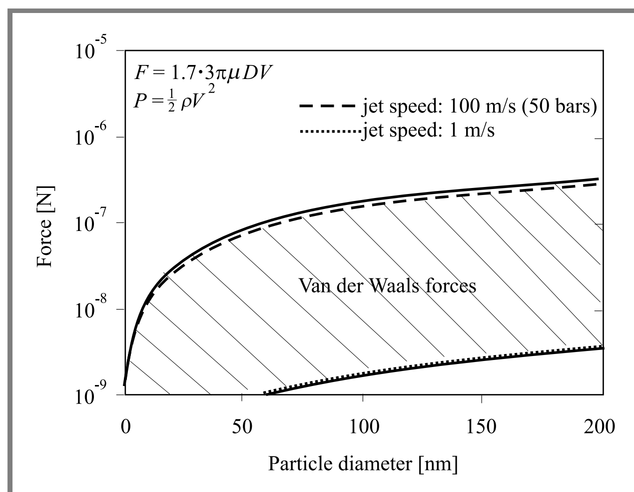

Fig. 9. Van der Waals and drag forces.

This cleaning method does not seem to be suitable for patterned wafers where particles are not accessible to the jet.

3.3. Cleaning by shock waves

The instantaneous overpressure induced by a shock wave (water hammer) on the cross section area of a particle generates a force likely to overcome the attractive van der Waals forces according to:

$$F_{shock} = \frac{\pi D^2}{4}\rho c V\,, \qquad (8)$$

where: D – particle diameter, ρ – mass density of the media, c – wave velocity in the media ($c = 1500$ m/s in water), V – speed of the media versus the particle.

Droplet jet. The particle removal process using a jet of droplets called “Soft Spray” has recently been proposed. It consists in spraying a mixture of liquid and gas onto

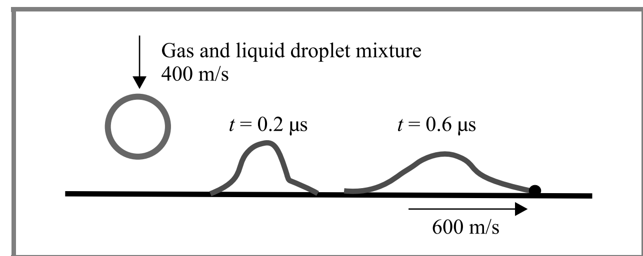

Fig. 10. Evolution of high velocity liquid droplet crashing at a perpendicular surface. Calculations taken from [13].

the wafer leading to a very high velocity heterogeneous jet. The generated droplet is projected onto the substrate with speeds in the range of 400 m/s. As represented in Fig. 10 calculations show that, when crashing, the droplet front even accelerates and strikes the particle at a speed of about 600 m/s [13]. Unlike a continuous jet, the exerted force is generated here by the shock wave from the droplet front applied to the particle surface.

Resonant acoustic cavitation. Cavitation in a liquid is due to the implosion of μ-bubbles after the loss of the equilibrium pressure conditions between the inside and outside the bubble:

$$P_{in} - P_{out} = \frac{4\gamma_{lg}}{D}\,, \qquad (9)$$

where: γ_{lg} – liquid/gas surface tension, D – bubble diameter.

The density of the energy liberated during bubble collapse is considerable as temperatures of 3000 K and pressures of 1000 atm are reached very locally. The bigger the bubble the higher the potential liberated energy. When a bubble collapses close to the surface, it can induce a microjet of liquid toward the surface that can reach a very high velocity of many hundreds of meters per second. This jet produces a very intense local shock wave. This phenomenon has been observed with a high-speed camera on bubbles in the mm range [14] and by nanosecond electrochemistry [15] with bubbles generated in an ultrasonic bath at 20 kHz. Acoustic cavitation has been observed in the megasonic range – up to 850 kHz – by sonoluminescence [16]. Nevertheless, it is not possible to conclude that the shock waves produced with megasonic frequencies that generate smaller bubbles are also induced by the same jet phenomenon.

As shown in Fig. 11, the periodic pressure wave variations generated in a sonic bath tend alternatively to increase and

decrease the bubble diameter to satisfy (9). Bubbles are initially present as germs in the media. When a bubble grows, its exchange surface increases, making the desorption of the dissolved gas present in the supersaturated liquid easier. In this way, during the successive pressure cycles, the bubbles grow until they reach the resonant size that depends on the acoustic wave frequency.

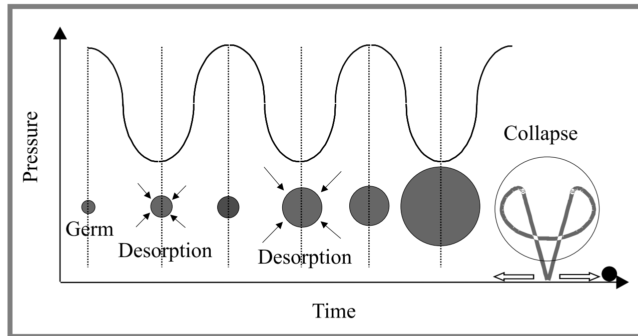

Fig. 11. Evolution of bubble sizes in an ultrasonic excitation until collapse (experimentally observed at the resonant size of the bubbles).

In water, neglecting the effects due to surface tensions and considering the transformations as adiabatic, the resonant frequency f_0 of bubbles is proportional to their radius R with a good approximation:

$$R_{[m]} f_{0[Hz]} \approx 3.26 \,. \tag{10}$$

Thus $R = 75$ μm at 40 kHz and 3 μm at 1 MHz.

At this frequency, the oscillation speed of the bubbles is maximum leading to the well known resonant cavitation phenomena observed in ultrasonic baths [17].
The megasonic efficiency strongly depends on the concentration and nature of the dissolved gas. High quantities of poorly soluble gas seem to be favorable for particle removal [18]. Acoustic wave transmission in the media is limited by the presence of big bubbles. Acoustic waves generate different streamings that prevent reattachment by carrying the removed particles far from the surface [19]. Extensive efforts still have to be made to understand the actual removal mechanisms occurring in megasonic baths.

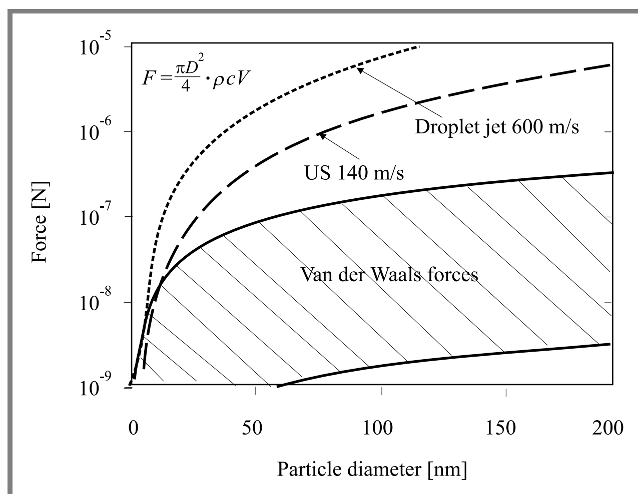

Fig. 12. Van der Waals and shock wave forces due to droplet jets and ultrasonic waves.

Cavitation is able to overcome van der Waals forces and, unfortunately, even to deteriorate the quality of the material. Using higher frequencies leads to smaller bubbles and consequently lower energies, which partly prevents material and pattern degradation but theoretically also decreases the removal forces for cleaning particles (limitation for the biggest size). Using a lower acoustic power leads to the same effect.
As shown in Fig. 12, the shock waves are theoretically able to remove all types and sizes of particles.

3.4. Cleaning using capillary forces

Capillary forces can potentially remove particles when they are located at the liquid/gas interface. This configuration is achieved, for example, during fast evaporation of a liquid phase or when wafers cross the liquid/gas interface of a bath.

Fast evaporation. This consists first in depositing a liquid medium at the wafer surface and then evaporating this liquid phase very quickly by decreasing the pressure (Fig. 13). The last fragments of the liquid can pull the particles off by the capillary force (or by simple mechanical drive). Different fluids have been envisaged, such as H_2O, CO_2, NH_3, ...

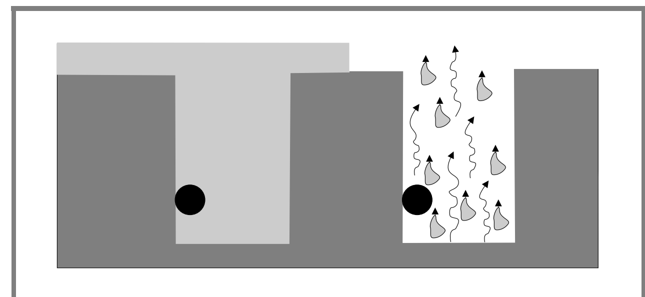

Fig. 13. Illustration of the cleaning principle by fast evaporation.

Bath interface. A.F.M. Leenaars [20] studied the capillary forces acting on a particle attached to a vertical substrate and located at the meniscus level of the air/liquid interface of a bath. In the particular case depicted in Fig. 14 (the liquid wets the substrate and not the particle), the maximum force is given by (11):

$$F_\gamma^{\max} = 2\pi R \gamma_{lg} \sin^2\left(\frac{\theta}{2}\right) \cos\alpha \,. \tag{11}$$

As seen in Fig. 15, theoretically, the capillary forces are not able to remove all types of particles, even in the favorable case of particles perfectly hydrophilic in water (a case of high surface tension).

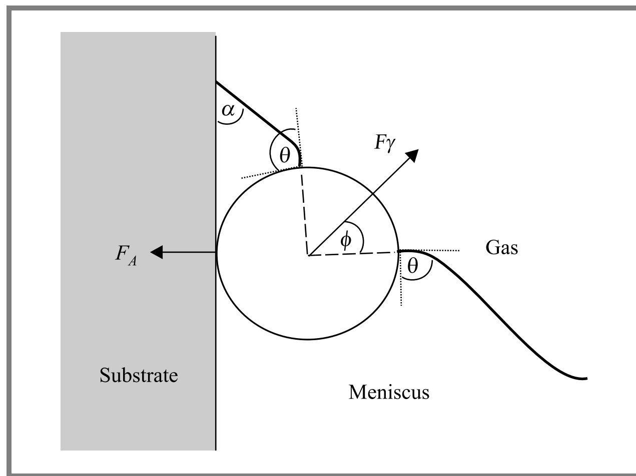

Fig. 14. Forces exerted on a particle attached to a substrate located at a gas/liquid interface.

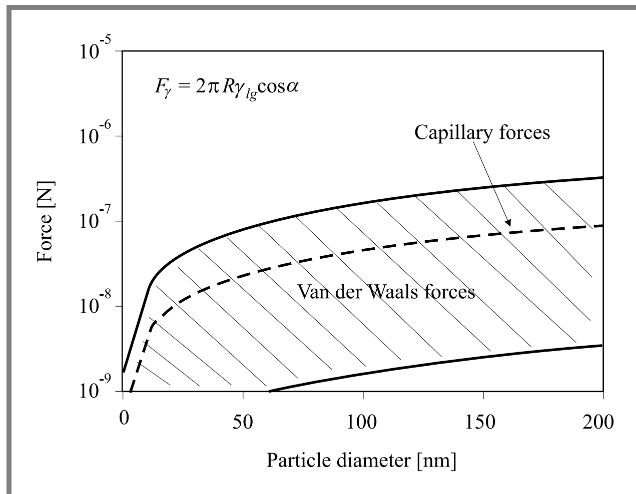

Fig. 15. Evolution of the van der Waals and maximum capillary forces (cos $\alpha = 1$, $\gamma_{lg} = 0.072$ N/m).

3.5. Cleaning using high acceleration

A very high acceleration due to the thermal expansion of the substrate and/or the particles heated up with a laser beam is likely to remove particles [21]. In this case, the force exerted on a particle of mass m is, in the first approach, given simply by:

$$F = m\gamma. \tag{12}$$

In practice, the acceleration is limited by the acceptable laser fluence leading to the melting of silicon. This threshold corresponds experimentally to the removal of the first alumina particles of about 100 nm (optimistic scenario). The corresponding acceleration calculated using Eq. (12) is in the 10^6 g range and thus higher than the one measured experimentally by Dobler *et al*. [22]. Anyway, as shown in Fig. 16, this method is not suitable for removing fine particles. To improve the removal capability of laser cleaning, a thin layer of liquid is first condensed from steam onto the substrate. In this case, the cleaning

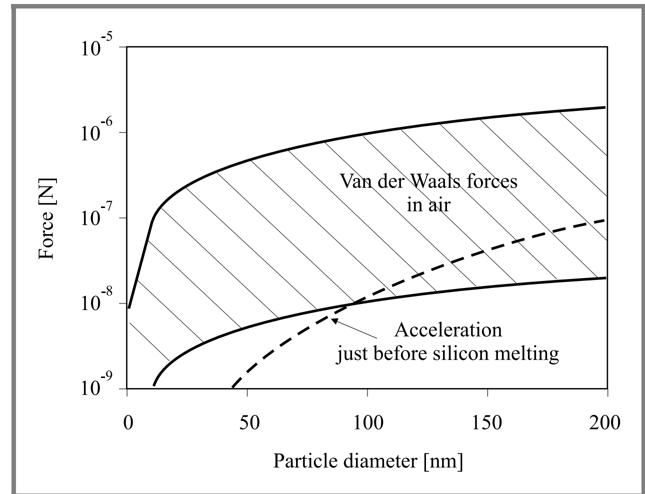

Fig. 16. Evolution of the van der Waals forces and the force generated by an acceleration able to remove the first 100 nm alumina particles, in air.

mechanism proposed by [21] would be close to the phenomenon of the cavitation process depicted above and consequently to its performance.

3.6. Cleaning by kinetic energy

In 1988, researchers at IBM Watson Research Center began to study cryogenic particle removal. This process uses the kinetic energy of a distribution of solid aerosol particles obtained for example by expansion cooling of gas such as Ar, N2, etc., [23]. This aerosol is then eliminated by sublimation. The particles just liberated are evacuated far from the substrate by thermophoresis or by a gaseous flow. If we consider that only one aerosol particle of mass m and velocity V reaches the particle at any one time, the removal condition is given by:

$$\int_{h_0}^{\infty} \frac{AR}{6h^2}\,\mathrm{d}h = \frac{AR}{12h_0} = \frac{1}{2}mV^2. \tag{13}$$

Collective effects may however occur.

In order to be able to remove particles located in lines and vias, the aerosol particles have to be smaller than the pattern dimensions.

4. Conclusion

In this work a range of van der Waals interactions covering 2 orders of magnitude is considered to take into account the majority of the variety of shapes and materials of the actual particles. This range has been determined by considering

the possible variations of the Hamaker constant and the difference between the ideal rigid sphere and real particles presenting finite contact areas, flattening effects, etc.
The different particle removal processes can be classified according to the physical effects used, such as electrostatic, drag and capillary forces, shock waves, acceleration, or kinetic energy. By comparing the attractive van der Waals forces and those generated by these effects it is then possible to predict the intrinsic capabilities and limitations of the different cleaning processes, particularly for the fine particles that have to be considered for the next IC generations. Three kinds of particle removal processes have been identified, namely universal processes able to remove all particle sizes and types even from patterned wafers, processes that present the same theoretical ability but are actually limited by the accessibility of the particles, and finally cleanings that are not able to remove all particle sizes.

- Particle removal by etching and electrostatic repulsion is the process used the most often through the SC1 cleaning step. This method does not seem to present any limitation in terms of particle size since the necessary material consumption is acceptable. In practice, this amount can be limited by increasing the etching speed, the ionic force of the solution and absolute values of Zeta potentials. It is also possible to remove all particle types by shock waves generated for example by megasonics in aqueous media. Nevertheless this method is limited by the erosion of the materials and by the mechanical resistance of the microstructures.
- High-speed aqueous jets, droplet jets, and aerosol sprays are theoretically able to remove all particle types accessible to the jet. Limitations arise from the mechanical resistance of the patterns and for particles hidden in the microstructures.
- Methods using capillary forces and high accelerations are not able to remove all particle types.

References

[1] International Technology Roadmap for Semiconductors, 2001, http://public.itrs.net/Files/2001ITRS/Home.htm

[2] W. Kern and D. Puotinen, "Cleaning solutions based on hydrogen peroxide for use in silicon semiconductor industry", RCA rev. 31, p. 187, 1970.

[3] F. Tardif, *Nettoyages par voie humide en micro-électronique dans l'ouvrage "Procédés de fabrication en micro-électronique"*. Hermes Science Publ., 2003.

[4] R. Comolet, *Mécanique expérimentale des fluides*. Tome II, 3rd ed. Paris: Masson, 1982.

[5] M. O'Neill, "A sphere in contact with a plane wall in a slow linear shear flow", *Chem. Eng. Sci.*, vol. 23, p. 1293, 1968.

[6] G. Ziskind, M. Fishman, and C. Gutfinger, "Resuspension of particulates from surfaces to turbulent flows. Review and analysis", *J. Aerosol Sci.*, vol. 26, pp. 613–644, 1995.

[7] J. Israelachvili, *Intermolecular & Surface Forces*. 2nd ed. Academic Press, 1997.

[8] P. C. Hiementz, *Principle of Colloid and Surface Chemistry*. 2nd ed. New York: Dekker Press, 1986.

[9] F. Tardif, I. Constant, R. J.-M. Pellenq, and A. Delville, "A new approach for particle removal based on a Monte Carlo simulation of electrostatic interactions", in *7th Int. Symp. Part. Surf.*, New York, USA, 2000.

[10] M. Meuris, P.-W. Mertens, A. Opdebeeck, H.-F. Schmidt, M. Depas, G. Vereecke, M.-M. Heyns, and A. Philipossian, "The IMEC clean: a new concept for particle and metal removal on Si surfaces", *Solid-State-Technol.*, vol. 38, no. 7, pp. 109-110, 112, 114, 1995.

[11] F. Tardif, T. Lardin, C. Paillet, J. P. Joly, A. Fleury, P. Patruno, D. Levy, and K. Barla, "Optimization of HF and oxidant wet cleanings before 7 nm gate oxide: introduction to "DDC": diluted dynamic clean", in *ECS*, Chicago, USA, 1995.

[12] F. Tardif, T. Lardin, B. Sandrier, P. Boelen, R. Matthews, I. Kashkoush, and R. Novak, "Performances of "DDC": diluted dynamic clean before 4.5 nm gate oxide", in *ECS*, Paris, France, 1997.

[13] N. Hirano, K. Takayama, J. Falcovitz, T. Katoaka, K. Shimada, and E. Ando, "Microscopic analysis of particle removal by gas/liquid mixture high-speed flow", in *UCPSS'98*, Oostende, Belgium, 1998.

[14] J. C. Isselin, A. P. Alloncle, and M. Autric, "On laser induced bubble near a solid boundary: contribution to the understanding of erosion phenomena", *J. Appl. Phys.*, vol. 84, no. 10, pp. 5766–5771, 1998.

[15] E. Maisonhaute, P. C. White, and R. G. Campton, "Surface acoustic cavitation understood via nanosecond electrochemistry", *J. Phys. Chem. B*, vol. 105, pp. 12087–12091, 2001.

[16] D. Zhang, "Fundamental study of megasonic cleaning". Ph.D. thesis, University of Minnesota, 1993.

[17] L. H. Thompson and L. K. Doraiswamy, "Sonochemistry: science and engineering", *Ind. Eng. Chem. Res.*, vol. 38, pp. 1215–1249, 1999.

[18] P. Besson, O. Keller, and G. Ching, "Particle removal evaluation in DI water with megasonic activation", in *Techn. Conf., Semicon. Eur.*, Munchen, Germany, 2002.

[19] A. Busnaina, J. Taylor, and I. Kashkoush, "Measurement of the adhesion and removal forces of sub micrometer particles on silicon substrates", *J. Adhes. Sci. Technol.*, vol. 7, p. 441, 1993.

[20] A. F. M. Leenaars, "Particles on surfaces I: detection, adhesion and removal", Ed. K. L. Mittal. New York: Plenum Press, 1988.

[21] X. Wu, E. Sacher, and M. Meunier, "The modeling of excimer laser particle removal from hydrophilic silicon surfaces", *J. App. Phys.*, vol. 87, no. 8, pp. 3618–3627, 2000.

[22] V. Dobler, R. Oltra, J. P. Boquillon, M. Mosbascher, J. Boneberg, and P. Leiderer, "Surface acceleration during dry laser cleaning of silicon", *Appl. Phys. Mat. Sci. & Proc. A*, vol. 69, pp. 335–337, 1999.

[23] J. J. Wu, D. Syverson, T. Wagner, and J. Weygand, "Wafer cleaning with cryogenic argon aerosols", in *Semicon. Int.*, Boise, USA, 1996.

François Tardif is the Head of the Ultra Clean Process Laboratory in the Microelectronics Department at CEA-Leti, Grenoble, France. He graduated from the engineering school of l'Institut National des Sciences Appliquées in Toulouse and received the Ph.D. degree in materials sciences from the University of Marseille, Marseille,

France. He is a member of the Electrochemical Society, he has co-organized congresses in the fields of silicon cleaning and ultra trace contamination measurements and has authored more than 50 papers.
e-mail: TardifFr@chartreuse.cea.fr
CEA Leti
17 rue des Martyrs
F-38054 Grenoble cedex 9, France

Adrien Danel received the diploma in engineering in 1994 and the Ph.D. degree in physics and microelectronics from the National Polytechnical Institute of Grenoble, France, in 1999. He is a research engineer at CEA Leti, working with silicon surface characterization by non-invasive methods and focusing on advanced cleaning processes.
e-mail: DanelAd@chartreuse.cea.fr
CEA Leti
17 rue des Martyrs
F-38054 Grenoble cedex 9, France

Olivier Raccurt received the B.Sc. degree in physics from the Université Claude Bernard, Lyon, France, in 2000, and the M.Sc. degree in materials science from the Institut National des Sciences Appliquées, Lyon, France, in 2001. He received the Ph.D. degree in physics and material science from the Université Aix-Marseille, Marseille, France, in 2004. This work was conducted at CEA Leti, Grenoble, France, and was focused on the mechanisms of stiction of microsystems during releasing step, involving studies on etching processes and cleaning of silicon substrate for micro-electronics, using atomic force microscopy for topological characterisation. He is currently holding a postdoctoral position at CEA Leti, where he is working on electrowetting on dielectric to move small droplets of biological liquid within the framework of a lab-on-chip project. His current research interests include the behaviour of liquid on solid at microscale dimension and atomic force microscopy characterisation.
e-mail: RaccurtOl@chartreuse.cea.fr
CEA Leti
17 rue des Martyrs
F-38054 Grenoble cedex 9, France